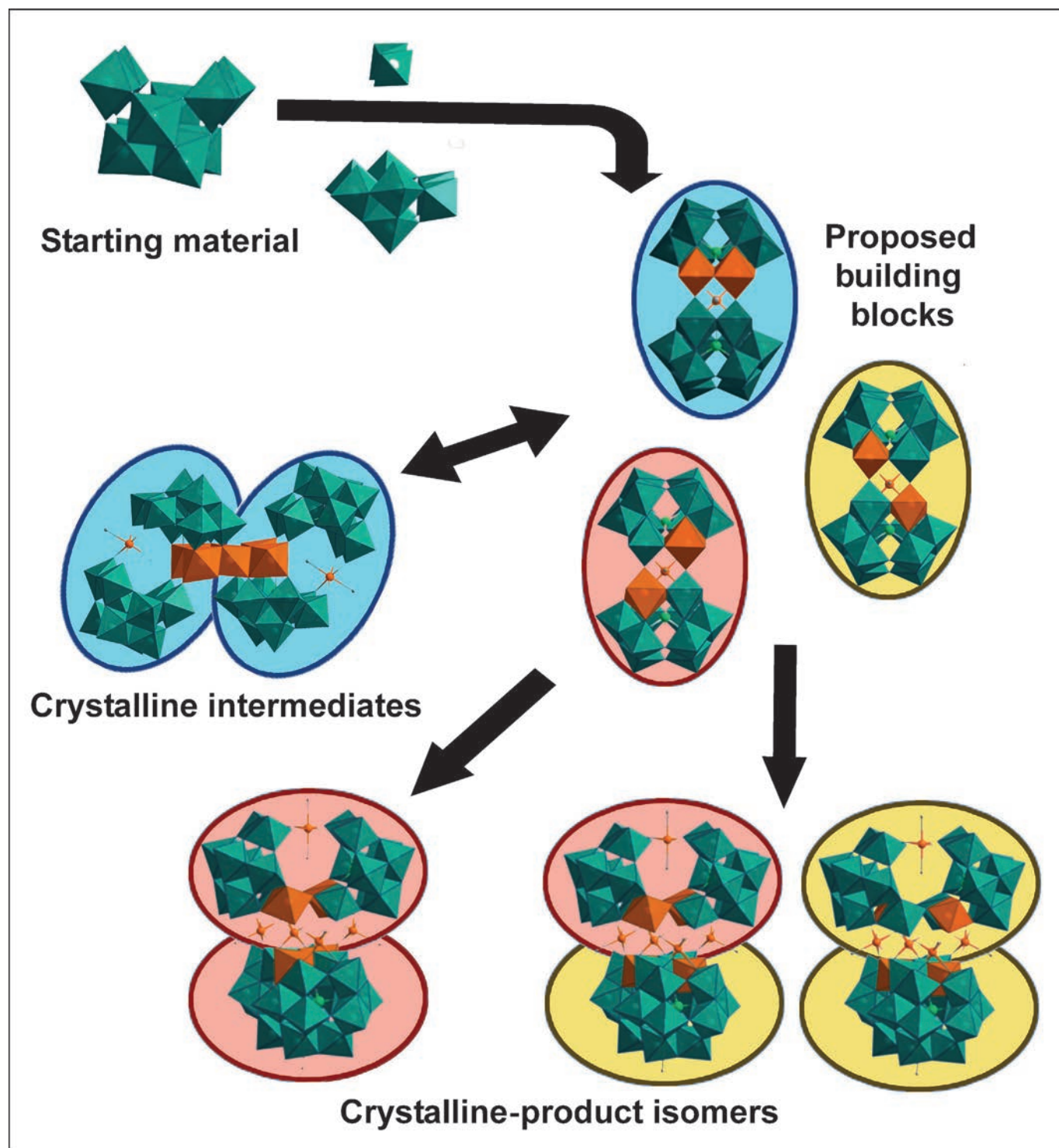


Nanoscale Control of Polyoxometalate Assembly: A $\{Mn_8W_4\}$ Cluster within a $\{W_{36}Si_4Mn_{10}\}$ Cluster Showing a New Type of Isomerism

Ross S. Winter,^[a] Jun Yan,^[a] Christoph Busche,^[a] Jennifer S. Mathieson,^[a]
Alessandro Prescimone,^[b] Euan K. Brechin,^[b] De-Liang Long,^[a] and Leroy Cronin*^[a]



Abstract: Two near isomeric clusters containing a novel $\{\text{Mn}_8\text{W}_4\}$ Keggin cluster within a $[\text{W}_{36}\text{Mn}_{10}\text{Si}_4\text{O}_{136}(\text{OH})_4(\text{H}_2\text{O})_8]^{24-}$ cluster are reported: $\text{K}_{10}\text{Li}_{14}[\text{W}_{36}\text{Si}_4\text{O}_{136}\text{Mn}_{10}(\text{OH})_4(\text{H}_2\text{O})_8]$ (**1**) and $\text{K}_{10}\text{Li}_{13.5}\text{Mn}_{0.25}[\text{W}_{36}\text{Si}_4\text{O}_{136}\text{Mn}_{10}(\text{OH})_4(\text{H}_2\text{O})_8]$ (**1'**). Bulk characterization of the clusters has been carried out by single crystal X-ray structure analysis, ICP-MS, TGA, ESI-MS, CV and SQUID-magnetometer analysis. X-ray analysis revealed that **1'** has eight positions within the central Keggin core that were disordered W/Mn whereas **1** contained no such disorder. This subtle

difference is due to a differences is how the two clusters assemble and recrystallize from the same mother liquor and represents a new type of isomerism. The rapid recrystallization process was captured via digital microscopy and this uncovered two “intermediate” types of crystal which formed temporarily and provided nucleation sites for the final clusters to assemble. The in-

termediates were investigated by single crystal X-ray analysis and revealed to be novel clusters $\text{K}_4\text{Li}_{22}[\text{W}_{36}\text{Si}_4\text{Mn}_7\text{O}_{136}(\text{H}_2\text{O})_8]\cdot 56\text{H}_2\text{O}$ (**2**) and $\text{Mn}_2\text{K}_8\text{Li}_{14}[\text{W}_{36}\text{Si}_4\text{Mn}_7\text{O}_{136}(\text{H}_2\text{O})_8]\cdot 45\text{H}_2\text{O}$ (**3**). The intermediate clusters contained different yet related building blocks to the final clusters which allowed for the postulation of a mechanism of assembly. This demonstrates a rare example where the use X-ray crystallography directly facilitated understanding the means by which a POM assembled.

Keywords: isomerization • pH control • polyoxometalates • self-assembly

Introduction

Transition-metal-substituted polyoxometalates (TMSPs) are of great interest due to their nanoscale size and tunable electronic and physical properties, for example, in such areas as catalysis, medicine, and materials science.^[1–5] Despite the ever increasing library of TMSPs, there has been little progress in understanding how isolated TMSP clusters are formed, and even less understanding of how to control aggregation to self-assemble “clusters-within-clusters” from lacunary precursors. Lacunary polyoxometalates are important, because they are vital building blocks used for the assembly of TMSPs owing to their nascent ability to rearrange readily in solution and to bind to transition metals in a variety of coordination modes.^[6–9] In particular, the lacunary polyoxotungstate $\text{K}_8[\gamma\text{-SiW}_{10}\text{O}_{36}]$, has shown enormous potential for the generation of unique TMSPs, such as $\text{K}_{18}[\text{Mn}^{\text{II}}_2\text{Mn}^{\text{III}}_4(\mu_3\text{-O})_2(\text{H}_2\text{O})_4(\text{B-}\beta\text{-SiW}_8\text{O}_{31})(\text{B-}\beta\text{-SiW}_9\text{O}_{34})(\gamma\text{-SiW}_{10}\text{O}_{36})]\cdot 40\text{H}_2\text{O}$ among others.^[10–13] Although considerable progress has been made in the controlled synthesis of TMSP clusters, interpretation of the self-assembly process often remains difficult due to the huge range of structures and coordination modes that can be achieved by simply adding transition-metal ions to lacunary POMs in solution resulting in a plethora of cluster types. Also, the disorder of doped transition-metal ions in large clusters presents a challenge in establishing the assembly mechanism, as well as routes to specifically position a given transition metal in a

specific site to engineer a particular magnetic, electronic, or catalytic feature.

Herein, we report the discovery and characterization of a high-nuclearity Mn containing TMSP cluster $\text{K}_{10}\text{Li}_{14}[\text{W}_{36}\text{Si}_4\text{O}_{136}\text{Mn}_{10}(\text{OH})_4(\text{H}_2\text{O})_8]$ (**1**), with a unique, highly substituted Keggin-type core $\{\text{H}_4\text{Mn}_8\text{W}_4\text{O}_{40}\}$ at its centre, such that the overall cluster is actually a cluster-within-a-cluster.

Importantly, the assembly of the cluster in a cluster at the nanoscale level allows the formation of an isomeric cluster with the same formula $\text{K}_{10}\text{Li}_{13.5}\text{Mn}_{0.25}[\text{W}_{36}\text{Si}_4\text{O}_{136}\text{Mn}_{10}(\text{OH})_4(\text{H}_2\text{O})_8]$ (**1'**), which differs only in the positions of the Mn centres captured in the precursor fragments, and thereby this system constitutes a new type of isomerism in metal oxide cluster science. This new “assembly isomerism” arises through combinatorial assembly at the building-block level with alternative combinations possible. Furthermore, all of the poly-anions are structurally derived from the $\{\gamma\text{-SiW}_9\}$ unit, which is reported herein for the first time. The molecular self-assembly process shows that the generation of $\{\gamma\text{-SiW}_9\}$ occurs not simply through direct degradation of $\{\gamma\text{-SiW}_{10}\}$, but also requires the assistance of the precursor $\{\beta\text{-SiW}_8\}$ building blocks. The generation of these types of “transient” building blocks is important, because it opens a new way of assembling far more complex cluster structures, especially if one transient building block is combined with another at the correct time in a multi-step one-pot reaction.^[14]

Results and Discussion

Synthesis and structural description of 1: The new poly-anion $[\text{W}_{36}\text{Si}_4\text{O}_{136}\text{Mn}_{10}(\text{OH})_4(\text{H}_2\text{O})_8]^{24-}$ (**1**) could be easily synthesized by a one-pot reaction of $\text{K}_8[\gamma\text{-SiW}_{10}\text{O}_{36}]$ precursor with Mn^{II} ions in a high-ionic-strength LiCl solution at pH 8.3 under ambient conditions, and isolated as orange

[a] R. S. Winter, Dr. J. Yan, Dr. C. Busche, Dr. J. S. Mathieson, Dr. D.-L. Long, Prof. L. Cronin
WestCHEM, School of Chemistry, The University of Glasgow
Glasgow G12 8QQ, Scotland (UK)
E-mail: lee.cronin@glasgow.ac.uk

[b] Dr. A. Prescimone, Prof. E. K. Brechin
EaStCHEM School of Chemistry, The University of Edinburgh
West Mains Road, Edinburgh, EH9 3JJ (UK)

Supporting information for this article is available on the WWW under <http://dx.doi.org/10.1002/chem.201204345>.

rod-shaped crystals in less than one day in approximately 13% yield (based on tungsten). Structural analysis of isomer **1** showed that there are a total of 46 available metal centres within the cluster, of which 36 positions are fully occupied by W and the ten other positions are occupied by Mn. Bond-valence-sum calculations showed that all the Mn ions are in the +2 oxidation state, and that the cluster contains four protons, which are located on the O atoms in the four Mn-O-Mn moieties within the central Keggin unit. The cluster can structurally be viewed as an eight-fold substituted Keggin cluster core encapsulated within four $\{\beta\text{-SiW}_8\}$ polyoxotungstate fragments and held together at the “poles” by a further two Mn centres as shown in Figure 1.

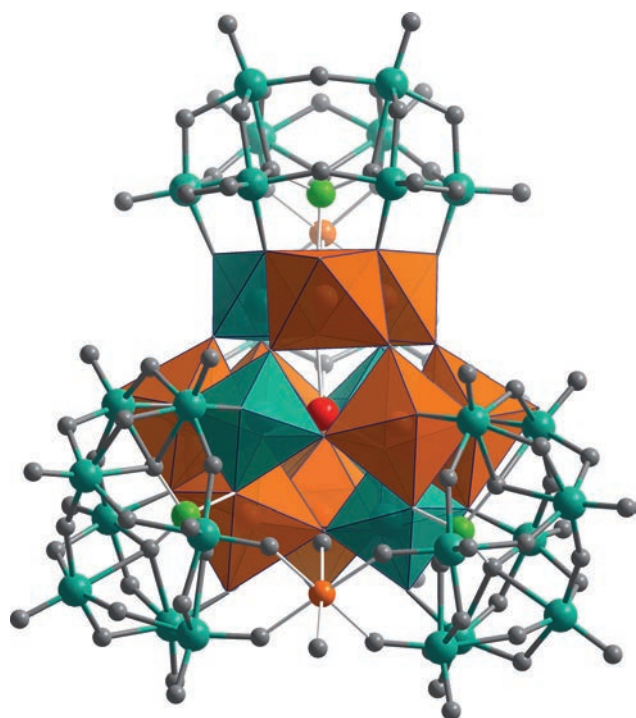


Figure 1. Structure of **1** $[\text{LiC}_{73}\text{W}_{36}\text{Si}_4\text{O}_{136}\text{Mn}_{10}(\text{OH})_4(\text{H}_2\text{O})_8]^{23-}$ highlighting the central Keggin motif. Colour scheme: W (dark green), Mn (orange), Li (red), Si (green), and O (grey).

Comparison of “assembly isomers” 1/1’: Further crystallographic studies lead to the isolation of an isomeric structure, **1’**. The difference between **1** and **1’** arises from the positional occupancy of tungsten and manganese within the Keggin core as shown in Figure 2. In compound **1**, each position of the Keggin is well defined as being either a Mn or W; however, in **1’** there is a level of disorder with four sites being crystallographically occupied by W/Mn 80:20% (purple in Figure 2) and four sites having an occupancy of W/Mn 20:80% (yellow in Figure 2). Interestingly, the positions occupied by 80% W in **1’** are fully occupied by Mn in **1**, and similarly the positions occupied by 80% Mn in **1’** are fully occupied by W in **1**, meaning that the cluster cages are approximate enantiomers. Overall, each cluster has a composition of 36 W/10 Mn and this ratio determined by X-ray anal-

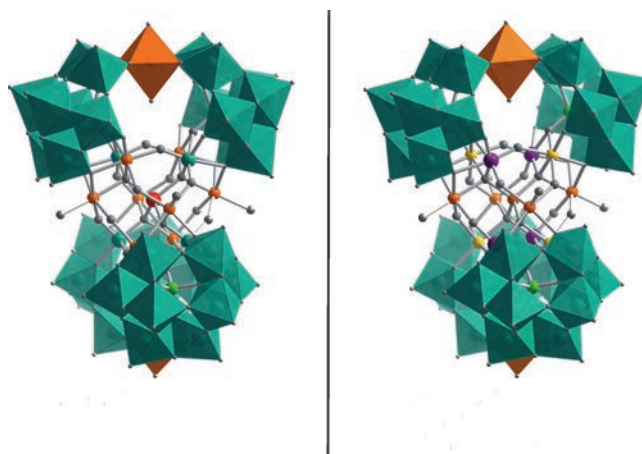


Figure 2. Comparison of the positional occupancy of Mn and W within the central Keggin unit of structures of **1** (left) and **1’** (right). Colour scheme: W/Mn 20:80% (purple), W/Mn 20:80% (yellow), W 100% (dark green): Mn 100% (orange). W- and Mn-based polyhedra are dark green and orange, respectively.

ysis has been corroborated by inductively coupled plasma (ICP) elemental analysis (see the Supporting Information). Another difference between the two structures arises from the atom situated at the centre of the Keggin core. In compound **1**, a lithium cation always acts as the central heteroatom of the Keggin core, whereas in **1’**, crystallographic analysis showed indications that the central position can be partially occupied by a manganese cation. Manganese-centred Keggin structures are very rare, however, a $\{\text{Mn}_{13}\}$ Keggin structure containing a central Mn^{IV} in an octahedral environment has been reported.^[13] In compound **1’**, the X-ray analysis indicated that the central Mn^{II} would be in a tetrahedral geometry, which would be the first example of such a heteroatom being found within a Keggin unit.

Mechanism of formation: The observation of “assembly isomers” **1** and **1’** can be attributed by the chelation to Mn^{II} cations of isomeric structural building blocks with the simplified formula $\{\text{Mn}_3\text{W}_{18}\text{Si}_2\}$ of which there are two identifiable forms (**a** and **b**). These structural building blocks are constructed from two $\{\gamma\text{-SiMnW}_9\}$ units and a $\text{Mn}^{\text{II}}(\text{H}_2\text{O})_2$ linker. The pairing of the $\{\text{Mn}_3\text{W}_{18}\text{Si}_2\}$ dimer building units can occur as the two homo-pairings (**aa/bb**) and the hetero-pairing (**ab**), which gives rise to the isomeric products. Structure **1**, with its well-defined Mn positions, is the product of one homo-pairing, whereas the disorder in structure **1’** can be attributed to a crystal mixture of the hetero-paired and other homo-paired building units. The assembly of clusters **1** and **1’** from $\{\gamma\text{-SiW}_{10}\}$ is illustrated in Figure 3 along with a schematic for the assembly isomerism. It is postulated that the driving force for the chelation of the building blocks can be attributed to the formation of a stabilized Keggin-type core.

Discovery of intermediate crystals: Although the high nuclearity Keggin core clusters **1** and **1’** were formed rapidly, two

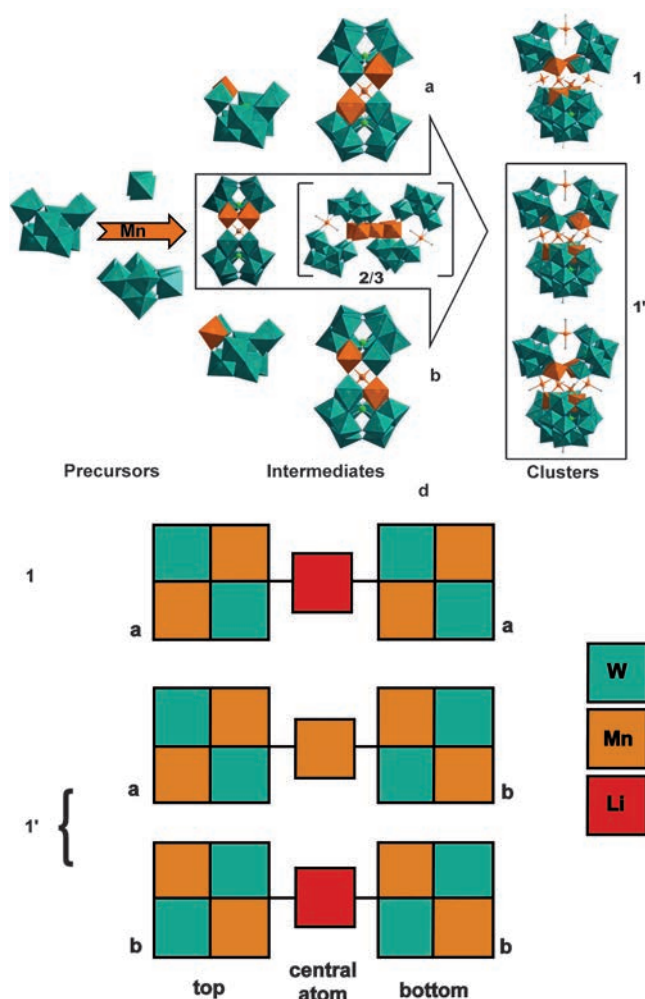


Figure 3. Top: proposed mechanism of assembly of **1** and **1'** via the step-wise assembly of building blocks and intermediates **2** and **3**, which are experimentally deduced structures. Full structural data are given in ref. [15]. The pairing of the $\{\text{Mn}_3\text{W}_{18}\text{Si}_2\}$ dimer building units can occur in three possible ways: two homo-pairings (**aa/bb**) and one hetero-pairing (**ab**). Bottom: schematic representation of how the isomerism is caused between **1** and **1'**.

types of intermediate crystals could still be detected during the crystallization process. Single-crystal X-ray analysis revealed structures **2** and **3**, which have common structural building units to **1** and **1'** (see the Supporting Information). As was discussed previously, the building units of **1** and **1'** are constructed of $\{\gamma\text{-SiMnW}_9\}$ units, whereas **2** and **3** are derived from building blocks comprising a $\{\gamma\text{-SiW}_{10}\}$ fragment and a di-manganese-substituted $\{\gamma\text{-SiMn}_2\text{W}_8\}$ fragment connected by a $\text{Mn}^{\text{II}}(\text{H}_2\text{O})_2$ linker. A similar $\{\text{W}_{10}\}/\{\text{W}_8\}$ substitution pattern has been observed before in the cluster $\text{K}_7[\text{Co}_{1.5}(\text{H}_2\text{O})_7][(\gamma\text{-SiW}_{10}\text{O}_{36})(\beta\text{-SiW}_8\text{O}_{30}(\text{OH}))\text{Co}_4(\text{OH})(\text{H}_2\text{O})_7]\cdot 36\text{H}_2\text{O}$.^[16]

Structure **2** is an S-shaped cluster with the generalized formula $\{\text{W}_{36}\text{Si}_4\text{Mn}_7\text{O}_{136}\}$, in which two of the dimeric building blocks are connected by an inserted Mn ion to give a core of five linked manganese ions. Structure **3** is an expansion of the S-shaped cluster of **2** into a 2D sheet through manga-

nese linkers that connect each cluster to six others. The linking manganese ions are attached onto the surface of the $\{\gamma\text{-SiMn}_2\text{W}_8\}$ units and not the $\{\gamma\text{-SiW}_{10}\}$, which is what prevents the structure expanding into three dimensions (see the Supporting Information for structures and crystallography).

Crystal growth: The crystal growth of clusters **1** and **1'** is particularly interesting when recorded visually by using a digital microscope. The initial crystals that form are yellow/orange blocks (**2**) and small yellow/orange rods (**3**). These crystals are only temporary, and after a number of hours, the sprouting of thicker rod-shaped crystals occurs on the block-shaped crystals of **2** (Figure 4). Growth of the larger

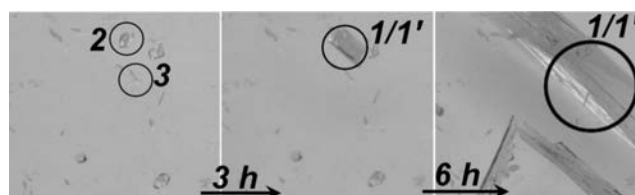


Figure 4. Time-lapsed growth of crystals of final products **1** and **1'** from intermediate crystals **2**.

crystals continues rapidly, consuming the initial block crystals in the process and forming layers of crystals of **1** and **1'**, and all these growth/dissolution processes allow us to follow assembly at the nano-molecular level by simply analysing single crystals of the compounds. A similar process occurs on the small rod crystals of **3**, however, at a slower rate and gives rise to micro-crystallites, which could not be analysed.

Based on the extraordinary optical and crystallographic observations, it can be hypothesized that the intermediate clusters are kinetic products, which are then superseded by the more stable products, **1** and **1'**. This hypothesis would support a mechanism, in which the $\{\gamma\text{-SiW}_{10}\}$ precursor first decomposes to $\{\beta\text{-SiW}_8\}$ (a similar mechanism has been proposed for the initial rearrangement of $\{\gamma\text{-GeW}_{10}\}$)^[17] and then the $\{\text{W}_{10}\}$ and $\{\text{W}_8\}$ fragments can combine rapidly leading to the formation of **2** and **3**. The $\{\gamma\text{-SiMnW}_9\}$ units, which serve as the building blocks for **1** and **1'**, are believed to be in equilibrium with the $\{\beta\text{-SiW}_8\}$ unit by recombination with aqueous Mn and W: thus, Mn can occupy one of two vacant positions leading to two isomeric forms. The equilibrium would be pushed in favour of the $\{\gamma\text{-SiMnW}_9\}$ fragments, because these can be stabilized through the formation of the central Keggin unit.

Further, a preliminary study of the solution behaviour of the nano-sized clusters, **1** and **1'**, has been conducted. A comparison of the MS (ESI) data by using single crystals of each cluster is shown in Figure 5. The clusters display very similar spectra, but it is possible to see distinct differences between **1** and **1'** in solution. The presence of highly charged peaks appearing above 1000 m/z range indicates that **1** and **1'** are stable as the parent cluster in such solutions. The pattern of cluster **1'** is slightly right shifted relative to **1**, which

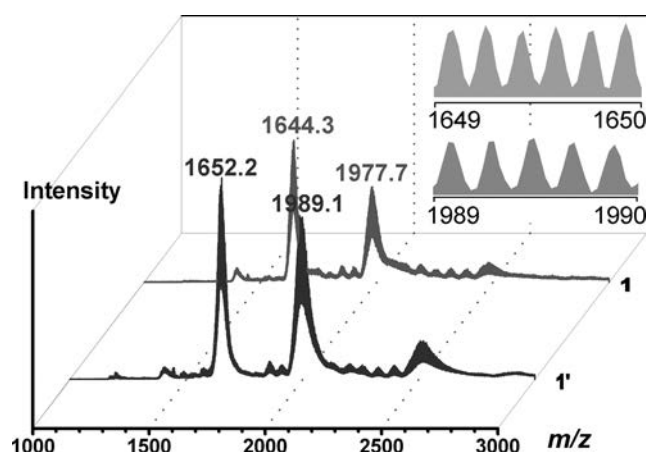


Figure 5. Comparative ESI-MS of clusters **1** and **1'**.

is consistent with the crystallographic observation of the Mn^{2+} at the centre of the embedded Keggin (cf. Li^+ in compound **1**). The two main signals for each cluster can be attributed to the -6 and -5 charged species with formulae $\{\text{KLi}_{18}[\text{W}_{36}\text{Si}_4\text{O}_{136}\text{Mn}_{10}(\text{OH})_4(\text{H}_2\text{O})_8](\text{H}_2\text{O})_4\}^{5-}$ at m/z 1977.7 and $\{\text{KLi}_{17}[\text{W}_{36}\text{Si}_4\text{O}_{136}\text{Mn}_{10}(\text{OH})_4(\text{H}_2\text{O})_8](\text{H}_2\text{O})_2\}^{6-}$ at m/z 1644.3 for **1** and $\{\text{K}_2\text{Li}_{16}\text{H}[\text{W}_{36}\text{Si}_4\text{O}_{136}\text{Mn}_{10}(\text{OH})_4(\text{H}_2\text{O})_8](\text{H}_2\text{O})_5\}^{5-}$ at m/z 1989.1 and $\{\text{KLi}_{16}\text{H}[\text{W}_{36}\text{Si}_4\text{O}_{136}\text{Mn}_{10}(\text{OH})_4(\text{H}_2\text{O})_8](\text{H}_2\text{O})_5\}^{6-}$ at m/z 1652.2 for **1'**, respectively. The assignments are in agreement with the formulae derived by crystallographic analysis.

Magnetic analysis: Magnetic-susceptibility measurements were performed on a powdered crystalline sample restrained in eicosane in the 5–275 K temperature range in an applied field of 0.1 T. The high-temperature χT value of $32.4 \text{ cm}^3 \text{ K mol}^{-1}$ is below that expected for 10 non-interacting Mn^{II} centres ($43.75 \text{ cm}^3 \text{ K mol}^{-1}$) and decreases with decreasing temperature to a minimum value of $9 \text{ cm}^3 \text{ K mol}^{-1}$ at 5 K. This behaviour indicates the presence of anti-ferromagnetic exchange between the metal centres with the 5 K value being that expected for two isolated $s=5/2$ paramagnets. The complexity of the magnetic core precludes any simple fit of the data. The χT versus T , M versus H and χ^{-1} versus T plots are given in the Supporting Information.

Conclusion

In conclusion, the formation of a new cluster within a cluster TMSP $[\text{W}_{36}\text{Si}_4\text{O}_{136}\text{Mn}_{10}(\text{OH})_4(\text{H}_2\text{O})_8]^{24-}$, which contains at its heart an octo-substituted manganese Keggin, has been reported. This cluster exists as two “assembly isomers”, which differ in the positions occupied by manganese within the central Keggin unit. The cluster displays the previously unseen $\{\gamma\text{-SiW}_9\}$ fragment as a structural building unit. We have tracked the crystal growth of this cluster and identified “intermediate” crystals, the X-ray structural analysis of which allowed us to map the assembly occurring directly in

solution for the first time. By careful examination of the crystal structures of the final and intermediate crystals and MS (ESI) analysis of the final clusters, we have been able to postulate a mechanism of formation, which not only explains the source of the “assembly isomerism” and why there are intermediate clusters, but also functions alongside and expands upon previously proposed mechanisms for the rearrangement of $\{\gamma\text{-XW}_{10}\}$ fragments in aqueous solution. This work has important perspectives for the assembly of polyoxometalates, because we are striving to control the assembly at the nanoscale and then translate this to larger scales, for example in the directed assembly of micron-scale architectures of polyoxometalate materials from molecular building blocks.^[18]

Experimental Section

Synthesis of 1 and 1': Freshly prepared $\text{K}_8[\gamma\text{-SiW}_{10}\text{O}_{36}]\cdot 12\text{H}_2\text{O}$ (1.45 g, 0.5 mmol) was dissolved in LiCl solution (30 mL, 4M). Anhydrous MnCl_2 (0.13 g, 1.0 mmol) was added to form a yellow solution. KOH (2M) was added drop-wise to raise the pH to 8.3, and then the pH was carefully sustained for 10 min by drop-wise addition of KOH (0.5M) as required. The solution became orange and turbid. The mixture was stirred for a further 30 min, and the solution became clear. The solution was centrifuged and filtered into a clean, wide-necked conical flask (50 mL) and left at 18 °C. Orange rod-shaped crystals of the clusters co-crystallized overnight. Yield: 210 mg, approximately 13% based on W (by using average weight of both clusters). Due to the similar size shape and colour of **1** and **1'**, manual separation was not possible, and bulk chemical analysis was conducted on mixtures of the two isomers. FTIR (powder): $\tilde{\nu} = 3337, 1624, 988, 937, 845, 760, 691, 637, 606 \text{ cm}^{-1}$; UV ($\lambda_{\text{max}}, \epsilon$): 352 nm, $7985 \text{ dm}^3 \text{ mol}^{-1} \text{ cm}^{-1}$; TGA was conducted on freshly prepared sample: water loss between 330 and 550 K was 11.54% (calcd 10.88%). The sample was dried in the desiccator for one week before MS (ICP) elemental analysis was conducted; elemental analysis calcd (%) for $\text{K}_{10}\text{Li}_{14}[\text{W}_{36}\text{Si}_4\text{O}_{136}\text{Mn}_{10}(\text{OH})_4(\text{H}_2\text{O})_8]\cdot 60\text{H}_2\text{O}$ ($M_w = 11239.42$) (**1**): W 58.92, Mn 4.88, K 3.47, Li 0.87; calcd for $\text{K}_{10}\text{Li}_{13.5}\text{Mn}_{10.25}[\text{W}_{36}\text{Si}_4\text{O}_{136}\text{Mn}_{10}(\text{OH})_4(\text{H}_2\text{O})_8]\cdot 60\text{H}_2\text{O}$ ($M_w = 11249.65$) (**1'**): W 58.87, Mn 5.01, K 3.46, Li 0.84; calcd average for both W 58.90, Mn 4.95, K 3.47, Li 0.86; found: W 63.82, Mn 5.14, K 3.56, Li 1.18 (consistent with a dried formula of $\text{K}_{10}\text{Li}_{14}[\text{W}_{36}\text{Si}_4\text{O}_{136}\text{Mn}_{10}(\text{OH})_4(\text{H}_2\text{O})_8]\cdot 13\text{H}_2\text{O}$).

Further details of the crystal structure investigation(s) can be obtained from the Fachinformationszentrum Karlsruhe, 76344 Eggenstein-Leopoldshafen, Germany (fax: (+49)7247-808-666; e-mail: crysdata@fiz-karlsruhe.de, http://www.fiz-karlsruhe.de/request_for_deposited_data.html) on quoting the depository number CSD-424731 (**1**), CSD-424732 (**1'**), CSD-424733 (**2**) and CSD-424734 (**3**).

Acknowledgements

We thank the EPSRC, WestCHEM, and University of Glasgow. L.C. thanks the Royal Society and Wolfson Foundation for a merit award.

- [1] M. Misono, *Chem. Commun.* **2001**, 1141–1152.
- [2] T. Yamase, *J. Mater. Chem.* **2005**, *15*, 4773–4782.
- [3] A. Proust, R. Thouvenot, P. Gouzerh, *Chem. Commun.* **2008**, 1837–1852.
- [4] D.-L. Long, R. Tsunashima, L. Cronin, *Angew. Chem.* **2010**, *122*, 1780–1803; *Angew. Chem. Int. Ed.* **2010**, *49*, 1736–1758.

- [5] K. Kamata, K. Yonehara, Y. Sumida, K. Yamaguchi, S. Hikichi, N. Mizuno, *Science* **2003**, *300*, 964–966.
- [6] S. G. Mitchell, C. Streb, H. N. Miras, T. Boyd, D.-L. Long, L. Cronin, *Nat. Chem.* **2010**, *2*, 308–312.
- [7] Z.-M. Zhang, Y.-G. Li, S. Yao, E.-B. Wang, *Dalton Trans.* **2011**, *40*, 6475–6479.
- [8] C. Lydon, C. Busche, H. N. Miras, A. Delf, D.-L. Long, L. Yellowlees, L. Cronin, *Angew. Chem.* **2012**, *124*, 2157–2160; *Angew. Chem. Int. Ed.* **2012**, *51*, 2115–2118.
- [9] P. Mialane, A. Dolbecq, J. Marrot, E. Rivière, F. Sécheresse, *Angew. Chem.* **2003**, *115*, 3647–3650; *Angew. Chem. Int. Ed.* **2003**, *42*, 3523–3526.
- [10] S. G. Mitchell, P. I. Molina, S. Khanra, H. N. Miras, A. Prescimone, G. J. T. Cooper, R. S. Winter, E. K. Brechin, D.-L. Long, R. J. Cogdell, L. Cronin, *Angew. Chem.* **2011**, *123*, 9320–9323; *Angew. Chem. Int. Ed.* **2011**, *50*, 9154–9157.
- [11] Y. Kikukawa, Y. Kuroda, K. Yamaguchi, N. Mizuno, *Angew. Chem.* **2012**, *124*, 2484–2487; *Angew. Chem. Int. Ed.* **2012**, *51*, 2434–2437.
- [12] a) Z. Zhang, Y. Li, E. Wang, X. Wang, C. Qin, H. An, *Inorg. Chem.* **2006**, *45*, 4313–4315; b) B. S. Bassil, U. Kortz, *Dalton Trans.* **2011**, *40*, 9649–9661.
- [13] G. N. Newton, S. Yamashita, K. Hasumi, J. Matsuno, N. Yoshida, M. Nihei, T. Shiga, M. Nakano, H. Nojiri, W. Wernsdorfer, H. Oshio, *Angew. Chem.* **2011**, *123*, 5834–5838; *Angew. Chem. Int. Ed.* **2011**, *50*, 5716–5720.
- [14] A. R. Oliva, V. Sans, H. N. Miras, J. Yan, H. Zang, C. J. Richmond, D.-L. Long, L. Cronin, *Angew. Chem.* **2012**, *124*, 12931–12934; *Angew. Chem. Int. Ed.* **2012**, *51*, 12759–12762.
- [15] Crystal data and structure refinements for **1**, **1'**, **2** and **3**: *Compound 1*: $\text{K}_{10}\text{Li}_{14}[\text{W}_{36}\text{Si}_4\text{O}_{136}\text{Mn}_{10}(\text{OH})_4(\text{H}_2\text{O})_8]\cdot 60\text{H}_2\text{O}$; $M_r = 11237.64 \text{ g mol}^{-1}$; block crystal: $0.31 \times 0.18 \times 0.14 \text{ mm}^3$; $T = 150(2) \text{ K}$; monoclinic, space group $C2/c$; $a = 40.395(4)$, $b = 18.3327(7)$, $c = 26.874(2) \text{ \AA}$, $\beta = 103.224(11)^\circ$, $V = 19374(6) \text{ \AA}^3$, $Z = 4$, $\rho = 3.853 \text{ g cm}^{-3}$; $\mu_{\text{MoK}\alpha} = 22.265 \text{ mm}^{-1}$; $F(000) = 20024$; 80451 reflections measured, of which 19023 are independent ($R_{\text{int}} = 0.0596$), 1113 re-
- fined parameters, $R_1 = 0.0583$ and $wR_2 = 0.1352$ (all data). *Compound 1'*: $\text{K}_{10}\text{Li}_{13.5}\text{Mn}_{0.25}[\text{W}_{36}\text{Si}_4\text{O}_{136}\text{Mn}_{10}(\text{OH})_4(\text{H}_2\text{O})_8]\cdot 60\text{H}_2\text{O}$; $M_r = 11247.91 \text{ g mol}^{-1}$; block crystal: $0.10 \times 0.08 \times 0.03 \text{ mm}^3$; $T = 150(2) \text{ K}$; monoclinic, space group $C2/c$, $a = 33.867(3)$, $b = 23.648(3)$, $c = 24.299(3) \text{ \AA}$, $\beta = 91.683(7)^\circ$, $V = 19452(4) \text{ \AA}^3$, $Z = 4$, $\rho = 3.841 \text{ g cm}^{-3}$; $\mu_{\text{MoK}\alpha} = 22.191 \text{ mm}^{-1}$; $F(000) = 20043$; 151970 reflections measured, of which 19096 are independent ($R_{\text{int}} = 0.179$), 1102 refined parameters, $R_1 = 0.0692$ and $wR_2 = 0.1885$ (all data). *Compound 2*: $\text{K}_4\text{Li}_{22}[\text{W}_{36}\text{Si}_4\text{Mn}_7\text{O}_{136}(\text{H}_2\text{O})_8]\cdot 56\text{H}_2\text{O}$; $M_r = 10753 \text{ g mol}^{-1}$; block crystal: $0.14 \times 0.08 \times 0.05 \text{ mm}^3$; $T = 150(2) \text{ K}$; triclinic, space group $P\bar{1}$, $a = 13.6468(7)$, $b = 18.6826(9)$, $c = 21.0946(9) \text{ \AA}$, $\alpha = 75.083(4)^\circ$, $\beta = 80.327(4)^\circ$, $\gamma = 77.804(4)^\circ$, $V = 5042.8(4) \text{ \AA}^3$, $Z = 1$, $\rho = 3.541 \text{ g cm}^{-3}$; $\mu_{\text{MoK}\alpha} = 21.076 \text{ mm}^{-1}$; $F(000) = 4765$; 66097 reflections measured, of which 17990 are independent ($R_{\text{int}} = 0.142$), 940 refined parameters, $R_1 = 0.0812$ and $wR_2 = 0.2315$ (all data). *Compound 3*: $\text{Mn}_2\text{K}_8\text{Li}_{14}[\text{W}_{36}\text{Si}_4\text{Mn}_7\text{O}_{136}(\text{H}_2\text{O})_8]\cdot 45\text{H}_2\text{O}$; $M_r = 10766.23 \text{ g mol}^{-1}$; block crystal: $0.15 \times 0.08 \times 0.05 \text{ mm}^3$; $T = 150(2) \text{ K}$; triclinic, space group $P\bar{1}$, $a = 12.6760(8)$, $b = 18.5485(12)$, $c = 20.7971(15) \text{ \AA}$, $\alpha = 88.087(5)^\circ$, $\beta = 79.021(5)^\circ$, $\gamma = 82.126(4)^\circ$, $V = 4754.9(4) \text{ \AA}^3$, $Z = 1$, $\rho = 3.760 \text{ g cm}^{-3}$; $\mu_{\text{MoK}\alpha} = 22.559 \text{ mm}^{-1}$; $F(000) = 4757$; 68298 reflections measured, of which 18564 are independent ($R_{\text{int}} = 0.125$), 1003 refined parameters, $R_1 = 0.0634$ and $wR_2 = 0.1679$ (all data).
- [16] a) L. Lisnard, P. Mialane, A. Dolbecq, J. Marrot, J. M. Clemente-Juan, E. Coronado, B. Keita, P. de Oliveira, L. Nadjó, F. Sécheresse, *Chem. Eur. J.* **2007**, *13*, 3525–3536; b) B. S. Bassil, M. H. Dickman, M. Reicke, U. Kortz, B. Keita, L. Nadjó, *Dalton Trans.* **2006**, 4253–4259.
- [17] N. H. Nsouli, A. H. Ismail, I. S. Helgadottir, M. H. Dickman, J. M. Clemente-Juan, U. Kortz, *Inorg. Chem.* **2009**, *48*, 5884–5890.
- [18] G. J. T. Cooper, R. W. Bowman, E. P. Magennis, F. Fernandez-Trillo, C. Alexander, M. J. Padgett, L. Cronin, *Angew. Chem.* **2012**, *124*, 12926–12930; *Angew. Chem. Int. Ed.* **2012**, *51*, 12754–12758.

Received: December 6, 2012

Published online: January 30, 2013